

Whole-body and Localized SAR and Dose Prediction Tool for Indoor Wireless Network Deployments

D. Plets*, W. Joseph*, K. Vanhecke*, G. Vermeeren*, S. Aerts*, M. Deruyck*, L. Martens*

* Information Technology Department, Ghent University/iMinds

Gaston Crommenlaan 8, B-9050 Ghent, Belgium

david.plets@intec.ugent.be

Abstract—In this paper, for the first time a tool is presented that allows the prediction of whole-body and localized Specific Absorption Rates (SARs) and absorbed doses for indoor network deployments. As an application, three scenarios are investigated, considering different network topologies for data traffic over WiFi and for phone call traffic over Universal Mobile Telecommunications System (UMTS). Also, the influence of phone call duration on the total absorbed dose is spatially and globally characterized. SARs and absorbed doses can be lowered when more base stations with a lower transmit power are installed. For the considered scenarios, a reduction by a factor 24 is observed for the downlink SAR in a WiFi deployment, and by a factor 2.4 for the uplink SAR in a UMTS deployment.

I. INTRODUCTION

Due to the increased use of indoor wireless networks and the concern about human exposure to radio-frequency (RF) sources, exposure awareness has increased during recent years. International organizations such as ICNIRP (International Commission on Non-Ionizing Radiation Protection) [1] have issued safety guidelines to limit the maximal electric-field strength due to wireless communications. Also on a national level, authorities have implemented laws and norms to limit the exposure to electromagnetic fields. A lot of research has been done on the characterization of RF exposure (e.g., [2]–[6]), and measurements have indicated that exposure in indoor environments cannot be neglected [7]. Most exposure studies however, merely focus on fields generated due to traffic from base station to user device (downlink (DL)), but in reality also the exposure due to the electromagnetic waves induced by the user device should be considered (uplink (UL)). Software tools for predicting the received signal quality [8]–[14] very often only focus on Quality of Service parameters, typically throughput, and do not account for exposure values.

In [15], the authors presented the WiCa Heuristic Indoor Propagation Prediction (WHIPP) tool, a set of heuristic planning algorithms, experimentally validated for network planning in indoor environments [15]. In [16], this tool was extended for automatic network planning satisfying exposure limits or even minimizing DL exposure in indoor wireless networks, without impairing coverage. In [17], it was further extended with prediction algorithms to simulate and visualize electric-field strengths due to DL traffic and localized Specific Absorption Rate (SAR) values due to UL traffic.

In this paper, instead of separating between UL (due to the mobile device's transmitted signal) and DL (due to the electric fields E originating from the base stations or APs) traffic,

exposure will be expressed as either a whole-body absorption due to both UL and DL or either a localized SAR_{10g} (SAR in 10 g tissue [7]) due to UL. The WHIPP tool will be extended with a feature to calculate these SAR values and visualize them on a ground plan of a building. Additionally, by setting the actual usage time, the tool will allow the calculation of localized and whole-body doses [18]. To the authors' knowledge, no network planning tools are yet available that spatially calculate SAR distributions nor absorbed doses.

Three scenarios (using either WiFi or Universal Mobile Telecommunications System (UMTS)) will be defined to investigate the influence of the number of base stations, power control, and uplink transmission duration on the exposure. In Section II, the WHIPP tool is discussed and how it is extended in this research. In Section III, the considered quantities are mathematically formulated. Section IV lists different scenarios of which the results are discussed in Section V. Finally, conclusions and future work are presented in Section VI.

II. WHIPP PREDICTION TOOL

The WiCa Heuristic Indoor Propagation Prediction (WHIPP) algorithm is a heuristic planning algorithm, developed and validated for the prediction of path loss in indoor environments [15]. It takes into account the effect of the environment on the wireless propagation channel and has been developed for the prediction of the path loss on a grid over an entire building floor or at specific locations. The granularity of the prediction is determined by the density of the grid points on the building floor. The algorithm bases its calculations on the determination of the dominant path between transmitter and receiver, i.e., the path along which the signal encounters the least obstruction. This approach is justified by the fact that more than 95% of the energy received is contained in only 2 or 3 paths [10]. The dominant path is determined with a multidimensional optimization algorithm that searches the lowest total path loss, consisting of a distance loss (taking into account the length of the propagation path), a cumulated wall loss (taking into account the walls penetrated along the propagation path), and an interaction loss (taking into account the propagation direction changes of the path, e.g., around corners). The model has been constructed for the 2.4 - 2.6 GHz band and its performance has been validated with a large set of measurements in various buildings [15]. In contrary to many existing tools no tuning of the tool's parameters is performed for the validation. Excellent correspondence between measurements and predictions is obtained, even for other buildings and floors [15]. The WHIPP tool contains a user interface that

was developed in collaboration with usability experts. This not only allows visualizing path loss, throughput or electric-field values, but based on the formulations presented in the next section, also power densities, (localized or whole-body) absorption values and doses.

III. MATHEMATICAL FORMULATION

A. Specific Absorption Rates

Whole-body and localized specific absorption rates SAR_{wb} and SAR_{10g} at a certain location are calculated as follows:

• **Whole-body SAR** SAR_{wb}^{DL} [W/kg] due to DL traffic from all base stations

$$SAR_{wb}^{DL} = \sum_{BS_i} \left(S_{BS_i} \cdot SAR_{REF_{wb}}^{DL-BS_{RAT_i}} \right), \quad (1)$$

where S_{BS_i} [W/m²] is the received power density due to base station BS_i (WiFi AP or UMTS femtocell) and $SAR_{REF_{wb}}^{DL-BS_{RAT_i}}$ [W/kg per W/m²] is the reference whole-body SAR (for 1 W/m² of received power density) due to BS_i using a certain Radio Access Technology (RAT). The power density S_{BS_i} can be calculated using the electric-field strength:

$$S_{BS_i} = \frac{E_{BS_i}^2 \cdot DC}{120 \cdot \pi}, \quad (2)$$

where E_{BS_i} [V/m] is the electric-field strength due to base station BS_i , observed at the considered location and with an assumed duty cycle of 100%. DC [-] is the actual duty cycle of the WiFi traffic generated by BS_i [19]. The duty cycle represents the relative transmission time of a signal. In WiFi, signals are not transmitted continuously and therefore the predicted power densities at 100% operation need to be multiplied by the duty cycle. For UMTS, the duty cycle is 100% for downlink.

• **Whole-body SAR** SAR_{wb}^{UL-MP} [W/kg] due to UL traffic from mobile phone MP towards base station BS_c it is connected to, using a certain radio access technology RAT

$$SAR_{wb}^{UL-MP} = P_{BS_c}^{MP-UL} \cdot DC \cdot SAR_{REF_{wb}}^{UL-MP_{RAT}}, \quad (3)$$

where $P_{BS_c}^{MP-UL}$ [W] is the MP's power transmitted towards the base station BS_c it is connected to, DC [-] is again the WiFi duty cycle of the UL traffic, and $SAR_{REF_{wb}}^{UL-MP_{RAT}}$ [W/kg per W] is the reference whole-body SAR (for 1 W of transmitted power) due to the MP operating at technology RAT. For UMTS, the duty cycle is 100% for uplink.

• **Localized SAR** SAR_{10g}^{UL-MP} [W/kg] in 10g tissue due to UL traffic from mobile phone MP towards base station BS_c it is connected to using a certain radio access technology RAT

$$SAR_{10g}^{UL-MP} = P_{BS_c}^{MP-UL} \cdot DC \cdot SAR_{REF_{10g}}^{UL-MP_{RAT}}, \quad (4)$$

with $P_{BS_c}^{MP-UL}$ [W] and DC [-] as defined above and $SAR_{REF_{10g}}^{UL-MP_{RAT}}$ [W/kg per W] the reference localized SAR_{10g} (for 1 W of transmitted power) due to the MP operating at technology RAT.

B. Absorbed doses

The whole-body dose D_{wb}^{total} [J/kg] [18], [20] at a certain location in a building is calculated as the sum of the whole-body dose D_{wb}^{DL} [J/kg] due to downlink and the whole-body dose D_{wb}^{UL-MP} [J/kg] due to the MP's uplink:

$$D_{wb}^{total} = D_{wb}^{DL} + D_{wb}^{UL-MP}, \quad (5)$$

To calculate these absorbed doses, the previously obtained SAR values need to be multiplied by the time duration of the exposure:

$$D_{wb}^{DL} = T_{total} \cdot SAR_{wb}^{DL}, \quad (6)$$

where T_{total} [s] is the time frame over which the absorbed dose is calculated, and

$$D_{wb}^{UL-MP} = T_{usage} \cdot SAR_{wb}^{UL-MP}, \quad (7)$$

where T_{usage} [s] the time duration of the connection of the MP with the base station.

The localized dose D_{10g} [J/kg] is calculated as follows:

$$D_{10g} = T_{usage} \cdot SAR_{10g}^{UL-MP}. \quad (8)$$

Note that for the localized absorption the contribution of the base station (DL) is assumed to be negligible. It is also important to note that the absorption due to the uplink transmission of *other* users is not accounted for in this paper.

C. Input parameters for SAR and dose calculations

The equations formulated above now allow calculating SAR values and absorbed doses. Some of the parameters however are required as input or need to be calculated by the WHIPP tool.

- In equation (2), E_{BS_i} (electric-field strength due to base station BS_i) can be calculated by the WHIPP tool as described in [16], [17].
- The **duty cycle** (in equations (2), (3), (4)) depends on the type and amount of traffic over the air [19]. In the following sections, simplified duty cycle value assumptions will be made, depending on the considered network topology.
- In equations (3) and (4), $P_{BS_c}^{Tx}$ (MP's power transmitted towards the base station) can also be calculated with the WHIPP tool as described in [17]. A fixed transmit power of 20 dBm is assumed for WiFi and a variable power for UMTS (due to power control).
- The **reference SAR values** from equations (3) and (4) are listed in Table I. The whole-body reference SAR

value for UMTS is obtained from [20] (cell phone placed to the right side of the head of the human model). The whole-body reference SAR value $SAR_{REF_{wb}}^{UL-MP_{RAT}}$ and localized $SAR_{REF_{10g}}^{UL-MP_{RAT}}$ values for WiFi for data usage are obtained through Finite-Difference Time-Domain (FDTD) simulations, where the mobile device is held in front of the body. The UMTS $SAR_{REF_{10g}}^{UL-MP_{RAT}}$ values are found in Federal Communications Commission (FCC) documents [21], [22]. The same mobile phone is assumed as in [17].

| RAT | $SAR_{REF_{wb}}^{DL-BS_{RAT}}$ [W/kg per W/m ²] | $SAR_{REF_{wb}}^{UL-MP_{RAT}}$ [W/kg per W] | $SAR_{REF_{10g}}^{UL-MP_{RAT}}$ [W/kg per W] |
|------|--|--|---|
| UMTS | 0.003 | 0.00495 | 2.075 |
| WiFi | 0.0028 | 0.0070 | 0.9497 |

TABLE I. REFERENCE WHOLE-BODY AND LOCALIZED SAR VALUES $SAR_{REF_{wb}}^{DL-BS_{RAT}}$, $SAR_{REF_{wb}}^{UL-MP_{RAT}}$, AND $SAR_{REF_{10g}}^{UL-MP_{RAT}}$ FOR WiFi AND UMTS, EXPRESSED IN W/KG PER 1 W TRANSMITTED POWER (UL) OR IN W/KG PER 1 W/m² OBSERVED POWER DENSITY (DL).

IV. SCENARIOS

Three scenarios will be investigated, one WiFi data scenario and two UMTS phone call scenarios. All scenarios are investigated in the office building depicted in Fig. 1. The building is 90 m long and 17 m wide and consists of concrete walls (grey) and layered drywalls (brown). For all scenarios, a receiver height of 130 cm above floor level is assumed.

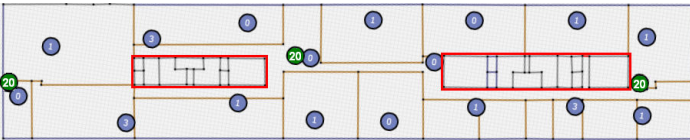


Fig. 1. WiFi network configurations for the traditional deployment (three APs with EIRP = 20 dBm, green dots) and for the exposure-optimized configuration (17 APs with EIRP between 0 and 3 dBm, purple dots). EIRP is indicated within dot

A. Scenario 1: SAR - WiFi/two network configurations

In a first scenario, two WiFi configurations will be compared based on their **whole-body and localized SAR**. The configurations are the ones from [16], in which a *traditional* network deployment (with maximal-power Equivalent Isotropically Radiated Powers (EIRPs)) and an *exposure-optimized* network deployment were compared based on only their electric-field strength distributions and based on a worst-case scenario with a duty cycle of 100%. Fig. 1 shows the two network deployments (in one figure). The traditional network deployment consists of the three 20-dBm green APs, the exposure-optimized deployment consists of the 17 low-EIRP purple APs. Both deployments were designed to provide the same throughput (**54 Mbps**). The locations where no coverage is required (kitchen, toilet, shed, elevator,...) are enclosed by the red rectangles. The APs are IEEE 802.11 b/g APs, operating on channel 1 (2412 MHz). For the downlink duty cycles, the assumption explained in [19] will be used. In the exposure-optimized configuration, the same amount of users is served by 5.66 (17/3) times as many APs, or, one AP needs to

serve 5.66 times fewer users. We assume that the downlink duty cycle for each AP is 6% for the exposure-optimized deployment and 34% (5.66 times 6%) for the traditional configuration. The uplink duty cycle will be assumed to be 2%, irrespective of the network configuration (duty cycles from [19]). Further research needs to be done to assess the influence of the number of users and their usage profiles on the actual duty cycle of an AP.

B. Scenario 2: SAR - UMTS/two network configurations

In the second scenario, similarly to the first scenario, two UMTS femtocell configurations will be compared based on their **whole-body and localized SAR**. The first configuration uses 1 UMTS femtocell base station (FBS) with an EIRP of 10 dBm to cover the entire building floor for **phone call coverage**, while the second configuration covers the floor with two UMTS FBSs with an EIRP of 0 dBm. In this UMTS scenario, the configuration with more FBSs (with a lower EIRP) will have the additional benefit of a lower average device transmit power due to power control [23], whereas for WiFi the MP's transmit power is fixed. Fig. 2 shows the two network deployments (in one figure). The traditional network deployment consists of one 10-dBm green FBS, the exposure-optimized deployment consists of two 0-dBm purple FBSs. Both deployments provide the same coverage (phone call coverage). The FBSs operate at a frequency of 2151.6 MHz for downlink traffic and 1957.6 MHz for uplink traffic. In the elevators, no phone call coverage is required. These are indicated in the figure by the red flags.

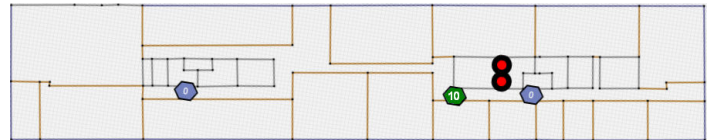


Fig. 2. UMTS network configurations for the traditional deployment (one FBS with EIRP = 10 dBm, green hexagon) and for the exposure-optimized configuration (2 FBSs with EIRP = 0 dBm, purple hexagon). EIRP is indicated within hexagon

C. Scenario 3: Absorbed doses - UMTS/two phone call durations

In a third scenario, the influence of the phone call duration (UL traffic) on the **total absorbed doses** is assessed for the UMTS femtocell **phone call** scenario from [17] and scenario 2. The network configuration with one femtocell from scenario 2 is investigated (green FBS in Fig. 2). Absorbed doses will be calculated for a one-hour time frame. In the first case, no phone call connection is made (no exposure due to UL), whereas in the second case, the user is calling the entire hour.

V. RESULTS

A. Scenario 1: WiFi - two network configurations

For the WiFi scenario, both configurations will cause the same uplink powers due to the absence of power control in WiFi devices: irrespective of the connection quality with the AP, a fixed power of 20 dBm is assumed. Table II indeed shows

that the SAR_{wb}^{UL-MP} and SAR_{10g}^{UL-MP} values are the same for the two configurations, $1.40 \cdot 10^{-5}$ and $1.90 \cdot 10^{-3}$ W/kg respectively. The downlink whole-body SAR SAR_{wb}^{DL} however, is drastically lowered in the exposure-optimized deployment, from $4.12 \cdot 10^{-8}$ to $1.71 \cdot 10^{-9}$ W/kg (a factor 24.1). Fig. 3 shows the spatial SAR_{wb}^{DL} distribution over the building floor. It illustrates the findings of Table II by showing the higher SAR_{wb}^{DL} for the traditional deployment with few high-EIRP APs (top) compared to the exposure-optimized deployment with many low-EIRP APs (bottom).

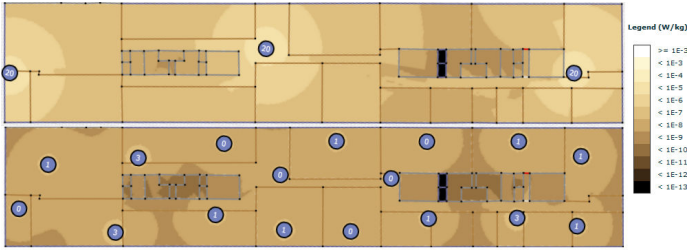


Fig. 3. SAR_{wb}^{DL} distribution for the traditional deployment (top) and for the exposure-optimized deployment (bottom) for scenario 1. AP EIRP is indicated within dot.

| Median SAR [W/kg] | | SAR_{wb}^{DL} | SAR_{wb}^{UL-MP} | SAR_{10g}^{UL-MP} |
|-------------------|---------|-----------------------|-----------------------|----------------------|
| Scenario 1 | Trad | $4.12 \cdot 10^{-8}$ | $1.40 \cdot 10^{-5}$ | $1.90 \cdot 10^{-3}$ |
| | Exp-opt | $1.71 \cdot 10^{-9}$ | $1.40 \cdot 10^{-5}$ | $1.90 \cdot 10^{-3}$ |
| Scenario 2 | Trad | $1.03 \cdot 10^{-9}$ | $8.56 \cdot 10^{-10}$ | $3.60 \cdot 10^{-7}$ |
| | Exp-opt | $2.60 \cdot 10^{-10}$ | $3.57 \cdot 10^{-10}$ | $1.50 \cdot 10^{-7}$ |

TABLE II. MEDIAN SAR VALUES FOR THE TWO SCENARIOS (WiFi AND UMTS) FOR TWO NETWORK CONFIGURATIONS.

B. Scenario 2: UMTS - two network configurations

Table II shows the whole-body and localized SAR values for two configurations defined in scenario 2 in Section IV. Similarly as in scenario 1, the whole-body DL absorption reduces when deploying more (lower-power) base stations (exposure-optimized) instead of fewer base stations with a higher EIRP (traditional): SAR_{wb}^{DL} reduces from $1.03 \cdot 10^{-9}$ to $2.60 \cdot 10^{-10}$ [W/kg] (a factor 4.0). In addition to a lower DL absorption, the exposure-optimized deployment with more base stations also allows taking advantage of the power control mechanism in UMTS. Due to the higher number of base stations, the MP will -on average- require a lower transmit power to maintain its connection. Table II shows that this also leads to a lower UL absorption: the whole-body uplink SAR and localized SAR are both reduced by a factor 2.4. Fig. 4, showing the spatial SAR_{wb}^{UL-MP} distribution over the building floor, illustrates this difference: SAR_{wb}^{DL} is higher for the traditional deployment with one FBS (top) compared to the exposure-optimized deployment with two FBSs (bottom). When comparing scenario 1 with scenario 2, it is clear that the SAR_{wb}^{DL} values are lower for UMTS, due to the less strict coverage requirement (high throughput vs. voice). This allows a network with fewer APs and/or APs with a lower EIRP. Thanks to the benefits of power control, the SAR_{wb}^{UL-MP} value (at least a factor 16355) and the SAR_{10g}^{UL-MP} (at least a factor 5278) value are much lower for the UMTS scenario than for the WiFi scenario.

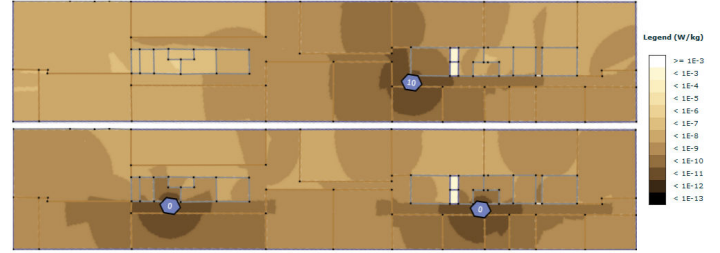


Fig. 4. SAR_{wb}^{UL-MP} distribution for the traditional deployment (top) and for the exposure-optimized deployment (bottom) for scenario 2. FBS EIRP is indicated within hexagon.

C. Scenario 3: UMTS - two phone call durations

Table III shows median whole-body and localized doses (D_{wb}^{DL} , D_{wb}^{UL-MP} , D_{wb}^{total} and D_{10g}) in one hour for the two phone call durations defined in scenario 3 in Section IV. The table shows that even when calling the entire time, the whole-body uplink dose ($3.08 \mu J/kg$) still remains below the whole-body dose due to the 10 dBm FBS ($3.71 \mu J/kg$). Fig. 5 shows the total whole-body dose in one hour for the two phone call duration: 0 s (top) and 3600 s (bottom). When no call is made (top), Fig. 5 shows that the total dose is only due to downlink (higher doses close to FBS). When the call lasts the entire hour, the total dose increases most near the cell edges, because the DL dose is the lowest and the UL dose the highest there. Close to the FBS, the total dose changes negligibly, due to the high DL dose and low UL dose. This leads to a more homogeneously distributed dose, as shown in Fig. 5 (bottom), with the highest doses very close to the FBS (DL dose high) and far from the FBS (leftmost rooms, UL dose high). The localized dose equals $540 \mu J/kg$ when calling for one hour.

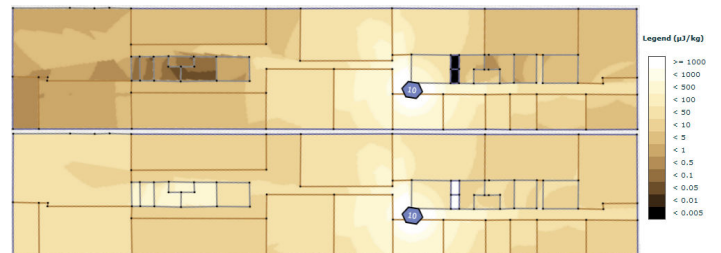


Fig. 5. D_{wb}^{total} distribution for a one-hour period when not calling (top) and when calling the entire hour (bottom). FBS EIRP is indicated within hexagon.

| Dose D [$\mu J/kg$] | | D_{wb}^{DL} | D_{wb}^{UL-MP} | D_{wb}^{total} | D_{10g} |
|-----------------------|---------|---------------|------------------|------------------|-----------|
| Scenario 3 | no call | 3.71 | 0 | 3.71 | 0 |
| | UMTS | 1-hour call | 3.71 | 3.08 | 6.79 |

TABLE III. DOSES IN ONE HOUR (LOCALIZED AND WHOLE-BODY) FOR SCENARIO 3 FOR TWO PHONE CALL DURATIONS.

VI. CONCLUSIONS AND FUTURE WORK

In this paper, a tool has been presented for the prediction of whole-body and localized SARs and absorbed doses for indoor wireless network deployments. The mathematical formulation has been given and three simulation scenarios were proposed. In a first scenario, it was shown that the whole-body SAR

due to WiFi downlink is reduced (by a factor 24) when using an exposure-optimized network deployment with many low-power access points. The second scenario showed that by adding base stations, also the uplink SAR is reduced for UMTS (by a factor 2.4), due to power control. In a third scenario, it was shown that for a traditional femtocell phone call deployment, UMTS downlink whole-body doses are still slightly higher than whole-body uplink doses when calling constantly. In future work, UMTS and WiFi will be mutually compared based on their spatial absorption distribution and a more accurate model for the determination of the duty cycle will be developed. Furthermore, exposure due to the uplink transmission of mobile devices of other users will be accounted for and Long-Term Evolution (LTE) will be considered.

ACKNOWLEDGMENT

This paper reports work undertaken in the context of the project LEXNET. LEXNET is a project supported by the European Commission in the 7th Framework Programme (GAN318273). For further information, please visit www.lexnet-project.eu.

REFERENCES

- [1] ICNIRP, "Guidelines for limiting exposure to time-varying electric, magnetic, and electromagnetic fields (up to 300 GHz)," *Health Physics*, vol. 74, no. 4, pp. 494–522, Apr. 1998.
- [2] K. R. Foster, "Radiofrequency exposure from wireless LANs using Wi-Fi technology," *Health Physics*, vol. 92, pp. 280 – 289, 2007.
- [3] W. Joseph, P. Frei, M. Roösli, G. Thuróczy, P. Gajsek, T. Trcek, J. Bolte, G. Vermeeren, E. Mohler, P. Juhsz, V. Finta, and L. Martens, "Comparison of personal radio frequency electromagnetic field exposure in different urban areas across Europe," *Environmental Research*, vol. 110, no. 7, pp. 658 – 663, 2010.
- [4] W. Joseph, P. Frei, M. Roösli, G. Vermeeren, J. Bolte, G. Thuróczy, P. Gajsek, T. Trcek, E. Mohler, P. Juhsz, V. Finta, and L. Martens, "Between-country comparison of whole-body SAR from personal exposure data in urban areas," *Bioelectromagnetics*, vol. 33, no. 8, pp. 682–694, December 2012.
- [5] P. Frei, E. Mohler, A. Bürgi, J. Fröhlich, G. Neubauer, C. Braun-Fahrlander, and M. Roosli, "A prediction model for personal radio frequency electromagnetic field exposure," *Science of The Total Environment*, vol. 408, no. 1, pp. 102 – 108, 2009.
- [6] A. Boursianis, P. Vantias, and T. Samaras, "Measurements for assessing the exposure from 3G femtocells," *Radiation Protection Dosimetry*, vol. 150, no. 2, pp. 158 – 167, 2012.
- [7] W. Joseph, L. Verloock, F. Goeminne, G. Vermeeren, and L. Martens, "Assessment of RF exposures from emerging wireless communication technologies in different environments," *Health Physics*, vol. 102, no. 2, pp. 161 – 172, February 2012.
- [8] Zhong Ji and Bin-Hong Li and Hao-Xing Wang and Hsing-Yi Chen and T.K. Sarkar, "Efficient ray-tracing methods for propagation prediction for indoor wireless communications," *IEEE Antennas and Propagation Magazine*, vol. 43, no. 2, pp. 41–49, April 2001.
- [9] R.P. Torres, L. Valle, M. Domingo, M.C. Diez, "CINDOOR: an engineering tool for planning and design of wireless systems in enclosed spaces," *IEEE Antennas and Propagation Magazine*, vol. 41, no. 4, pp. 11–22, Sept. 1999.
- [10] G. Wlflé, R. Wahl, P. Wertz, P. Wildbolz, and F. Landstorfer, "Dominant path prediction model for indoor scenarios," in *German Microwave Conference (GeMIC)*, Ulm, Germany, April 2005.
- [11] A.G. Dimitriou and S. Siachalou and A. Bletsas and J.N. Sahalos, "An Efficient Propagation Model for Automatic Planning of Indoor Wireless Networks," in *3rd European Conference on Antennas and Propagation*, Barcelona, Spain, 12-16 April 2010.
- [12] P. Sebastiao, R. Tome, F. Velez, A. Grilo, F. Cercas, D. Robalo, A. Rodrigues, F. F. Varela and C. X. P. Nunes, "WLAN Planning Tool: a Techno-Economic Perspective," in *COST 2100 TD(09)935 meeting*, Vienna, Austria, 28-30 September 2009.
- [13] S. Phaiboon, "An empirically based path loss model for indoor wireless channels in laboratory building," in *TENCON '02. Proceedings. 2002 IEEE Region 10 Conference on Computers, Communications, Control and Power Engineering*, vol. 2, October 2002, pp. 1020–1023.
- [14] J.M. Keenan and A.J. Motley, "Radio Coverage in Buildings," *BTSJ*, vol. 8, no. 1, pp. 19–24, January 1990.
- [15] D. Plets, W. Joseph, K. Vanhecke, E. Tanghe, and L. Martens, "Coverage Prediction and Optimization Algorithms for Indoor Environments," *EURASIP Journal on Wireless Communications and Networking, Special Issue on Radio Propagation, Channel Modeling, and Wireless, Channel Simulation Tools for Heterogeneous Networking Evaluation*, vol. 1, 2012. [Online]. Available: <http://jwcn.eurasipjournals.com/content/2012/1/123>
- [16] D. Plets, W. Joseph, K. Vanhecke, and L. Martens, "Exposure Optimization in Indoor Wireless Networks by Heuristic Network Planning," *Progress In Electromagnetic Research (PIER)*, vol. 139, pp. 445–478, 2013.
- [17] D. Plets, W. Joseph, S. Aerts, K. Vanhecke, and L. Martens, "Prediction and Comparison of Downlink Electric-Field and Uplink Localized SAR Values for Realistic Indoor Wireless Network Planning," *Radiation Protection Dosimetry*, February 2014.
- [18] S. Aerts, D. Plets, L. Verloock, W. Joseph, and L. Martens, "Assessment and Comparison of RF EMF Exposure in Femtocell and Macrocell Scenarios," *Bioelectromagnetics*, accepted.
- [19] W. Joseph, D. Pareit, G. Vermeeren, D. Naudts, L. Verloock, L. Martens, and I. Moerman, "Determination of the duty cycle of WLAN for realistic radio frequency electromagnetic field exposure assessment," *Progress in Biophysics & Molecular Biology*, October 2012.
- [20] O. Lauer, P. Frei, M. Gosselin, W. Joseph, M. Roosli, and F. J., "Combining near-and far-field exposure for an organ-specific and whole-body rf-emf proxy for epidemiological research: a reference case," *Bioelectromagnetics*, vol. 34, no. 5, pp. 366–374, 2013.
- [21] "Federal Communications Commission. Office of Engineering and Technology." Tech. Rep., last accessed on Dec 19, 2013. [Online]. Available: [url = https://apps.fcc.gov/oeetcf/eas/reports/ViewExhibitReport.cfm?mode=Exhibits&calledFromFrame=N&application_id=922267](https://apps.fcc.gov/oeetcf/eas/reports/ViewExhibitReport.cfm?mode=Exhibits&calledFromFrame=N&application_id=922267)
- [22] "Federal Communications Commission. Office of Engineering and Technology." Tech. Rep., last accessed on Dec 19, 2013. [Online]. Available: [url = https://apps.fcc.gov/oeetcf/eas/reports/ViewExhibitReport.cfm?mode=Exhibits&calledFromFrame=N&application_id=456890](https://apps.fcc.gov/oeetcf/eas/reports/ViewExhibitReport.cfm?mode=Exhibits&calledFromFrame=N&application_id=456890)
- [23] 3rd Generation Partnership Project, "UTRA (UE) FDD; Radio transmission and Reception, TS 25.101," Tech. Rep. [Online]. Available: <http://www.3gpp.org/specs/specs.htm>